Electronic supplementary information

Accelerating Electrosynthesis of Ammonia from Nitrates Using Coupled NiO/Cu Nanocomposites

Hongbo Zhu,[ab] Yanfeng Tang,[c] Jiacheng Jayden Wang,[b] Tongming Sun,[c] Minmin Wang,[c] Jin Wang,[c] Yongwen Tan,[a]* and Jiacheng Wang [bd]*

[a] College of Materials Science and Engineering, Hunan University, Changsha, Hunan 410082, China

[b] State Key Laboratory of High Performance Ceramics and Superfine Microstructure, Shanghai Institute of Ceramics, Chinese Academy of Sciences, Shanghai 201899, China

[c] School of Chemistry and Chemical Engineering, Nantong University, Nantong 226019, Jiangsu, China.

[d] School of Materials Science and Engineering, Taizhou University, Taizhou 318000, Zhejiang, China

Email: jiacheng.wang@mail.sic.ac.cn; tanyw@hnu.edu.cn

EXPERIMENTAL SECTION:

Chemicals and reagents

Nickel nitrate hexahydrate ($Ni(NO_3)_2 \cdot 6H_2O$), copper nitrate trihydrate ($Cu(NO_3)_2 \cdot 3H_2O$), ammonium chloride (NH_4Cl), ethanol (C_2H_5OH), potassium nitrate (KNO_3), potassium nitrite (KNO_2), hydrochloric acid (HCl), potassium hydroxide (KOH) and Nesser's reagent were purchased from Sinopharm Chemical Reagent Co., LTD. All reagents were received as the analytical grade and used without any purification.

Pretreatment of Cu foam (CF)

Pieces of CFs（1×1 cm^2）were cleaned in an ultrasonic bath of 0.1 mol/L HCl for 10 min to remove the oxides on the surface. Then, they were washed using deionized water and absolute ethanol in sequence under ultrasonication. Wet CF is preserved by immersion in refresh absolute ethanol at room temperature.

Synthesis of NiO/Cu

After cleaning, the CF was dried in a vacuum drying oven at a temperature of 80°C for 12 hours. Then, it was heated in a tube furnace at a rate of 3°C/min in an air atmosphere until reaching a temperature of 400 °C. The heating was maintained for a duration of 3 hours to obtain CuO nanowires (NWs). The CuO NWs was used as the working electrode, the parallel carbon rod was used as the counter electrode, and calomel was used as the reference electrode. The Cu NWs were obtained by electrochemical reduction of CuO NWs at -0.6 V vs. RHE in a standard three-electrode electrochemical cell for 30 min. Then, the co-electric deposition was performed in a standard three-electrode electrochemical cell with Cu NWs as the working electrode, parallel-placed carbon rods as the opposite electrode, and calomel as the reference electrode. The electrolyte consists of XNO_3（X = Ni, Fe, Co）and $Cu(NO_3)_2 \cdot 3H_2O$ dissolved in 100 ml deionized water with a stoichiometric number of 5.5 mmol. Constant current electrodeposition was then carried out at -100 mA at 25 °C. The deposition time for synthesize NiO/Cu is 15 minutes. After co-electric deposition, NiO/Cu and other nanocomposites were carefully removed from the electrolyte, rinsed with water and ethanol, and then dried overnight at 60 °C.

Structural and surface characterization

Scanning electron microscopy (SEM) images were collected on a field emission scanning electron microscope (FEI Magellan 400 L XHR). Transmission electron microscopy (TEM), high-resolution TEM (HRTEM), high-angle annular darkfield scanning TEM (HADDF-STEM) and energy-dispersive X-ray spectroscopy (EDS) mapping were obtained on the Titan G 260-300. Surface composition and chemical state were revealed by thermodynamic X-ray photoelectron spectroscopy (XPS) measurements using an AXIS ULTRA DLD electron spectrometer (voltage: 15 kV, current: 10 mA, full spectrum flux: 160, narrow spectrum flux: 40, monochromatic aluminum target). X-ray diffraction (XRD) measurements were performed on the Bruker D8 ADVANCE X-ray diffractometer.

Electrochemical measurements

All measurements were performed at 25 °C in an H-type electrolyzer using a CHI 760 E electrochemical workstation. In the three-electrode electrochemical cell, the prepared material was used as the working electrode (1 cm × 1 cm), the carbon rod was used as the counter electrode, and the calomel electrode was used as the reference electrode. Fumasep FAB-PK-130 was used as an anion exchange membrane. All potentials in this paper were converted to the potentials vs. reversible hydrogen electrode (RHE) through the equation $E_{RHE}=E_{SCE}+0.244+0.0592pH$. The NO_3RR and NO_2RR performances of the catalytic materials were tested in 1 M KOH with 0.1M KNO_3/0.1M KNO_2 by linear sweep voltammetry (LSV) with a scanning rate of $5mV\cdot s^{-1}$. The specific test conditions for EIS are as follows: the starting voltage (V) is the voltage corresponding to 10 $mA\cdot cm^{-2}$, the high frequency (Hz) is 100,000, the low frequency (Hz) is 1, the amplitude (V) is 0.005, and the quiet time (sec) is 2 seconds.

Detection of NH_4^+

The quantification of NH_4^+ was conducted with Nessler's reagent as the coloring agent. 0.2 mL electrolyte after NO_3^-RR was first taken out from the cathodic compartment and diluted to 5 mL. Then, potassium sodium tartrate solution (500 g L^{-1}, 0.1 mL) was added and thoroughly mixed. In the last step, 0.1 mL of Nessler's reagent was added to the above mixture. After being left standing for 20 min, the absorbance at 420 nm was measured by UV-spectroscopy (PG200-Pro back-thinned spectrometer,

ideaoptics, China). The obtained value was then fitted to the calibration curve to acquire the corresponding NH_4^+ concentration.

The NH_4^+ was calculated as follows:

Yield $NH_4^+ = (C_{NH4+} \times V) / (t \times S)$

The Faradaic efficiency was calculated as follows:

Faradaic efficiency = $(8F \times C_{NH4+} \times V) / (M_{NH4+} \times Q)$

where C_{NH4+} is the mass concentration of NH_4^+(aq), V is the volume of electrolyte in the cathode compartment, t is the electrolysis time, S is the geometric area of working electrode, F is the Faraday constant (96485 $C \cdot mol^{-1}$), M_{NH4+} is the molar mass of NH_4^+, and Q is the total charge passing the electrode.

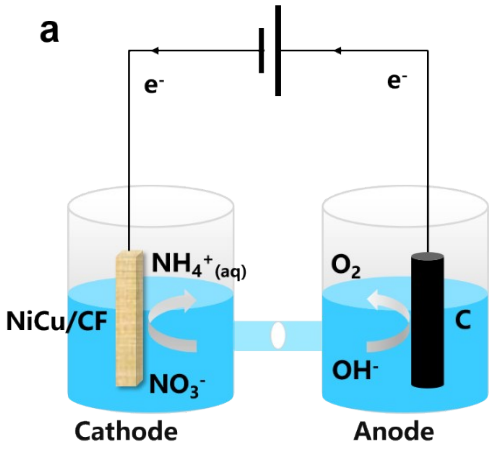

$NO_3^-{}_{(aq)} \rightarrow NO_3^-{}_{(ads)}$ (1)

$NO_3^-{}_{(ads)} + 2H_{(ads)} \rightarrow NO_2^-{}_{(ads)} + 2OH^-$ (2)

$NO_2^-{}_{(ads)} + H_{(ads)} \rightarrow NO^-{}_{(ads)} + OH^-$ (3)

$NO^-{}_{(ads)} + H_{(ads)} \rightarrow N^-{}_{(ads)} + OH^-$ (4)

$N^-{}_{(ads)} + H_{(ads)} \rightarrow NH_{(ads)}$ (5)

$NH_{(ads)} + H_{(ads)} \rightarrow NH_{2(ads)}$ (6)

$NH_{2(ads)} + H_{(ads)} \rightarrow NH_{3(ads)}$ (7)

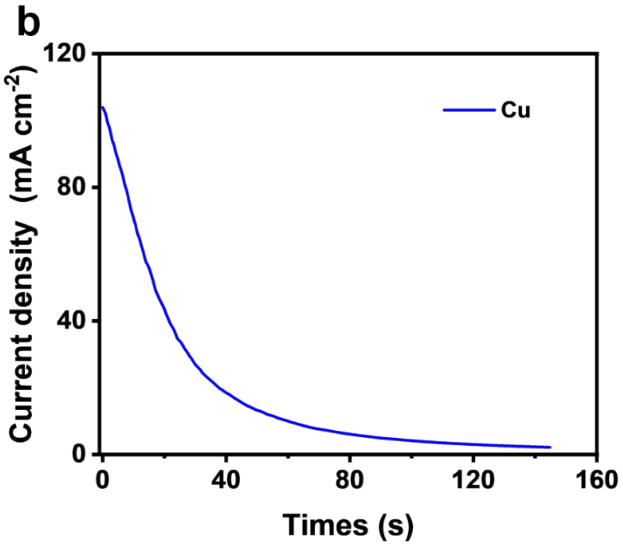

Figure S1a. Schematic showing the conversion of waste NO_3^- (from industry and agriculture) to NH_3 via the electrochemical nitrate reduction reaction (NO_3RR) pathway with relevant reaction steps. b, The poisoning phenomenon of Cu

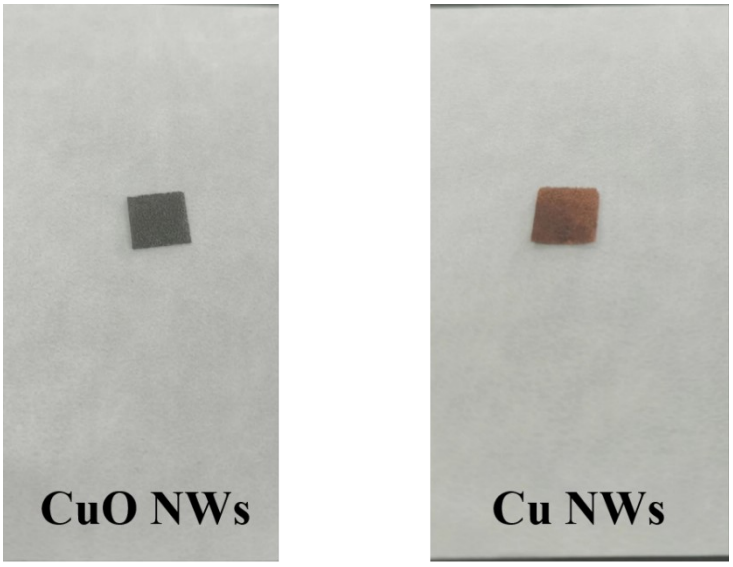

Figure S2. (left) CuO NWs on CF prepared by heattreatment of CF in air at 400 °C and (right) the Cu NWs on CF prepared by electro-reduction of CuO NWs on CF

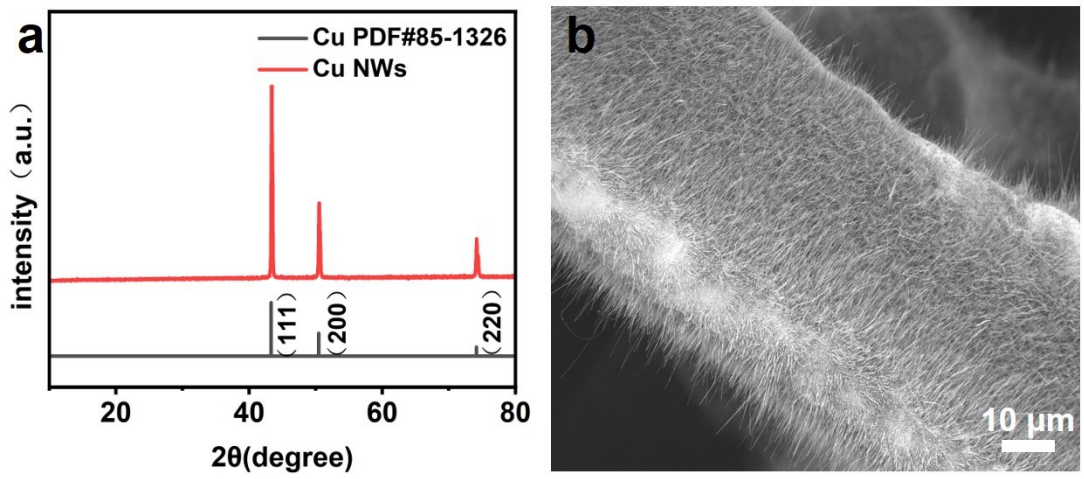

Figure S3. a) XRD image of the CuO NWs obtained by reduction.; b) SEM image of CuO NWs.

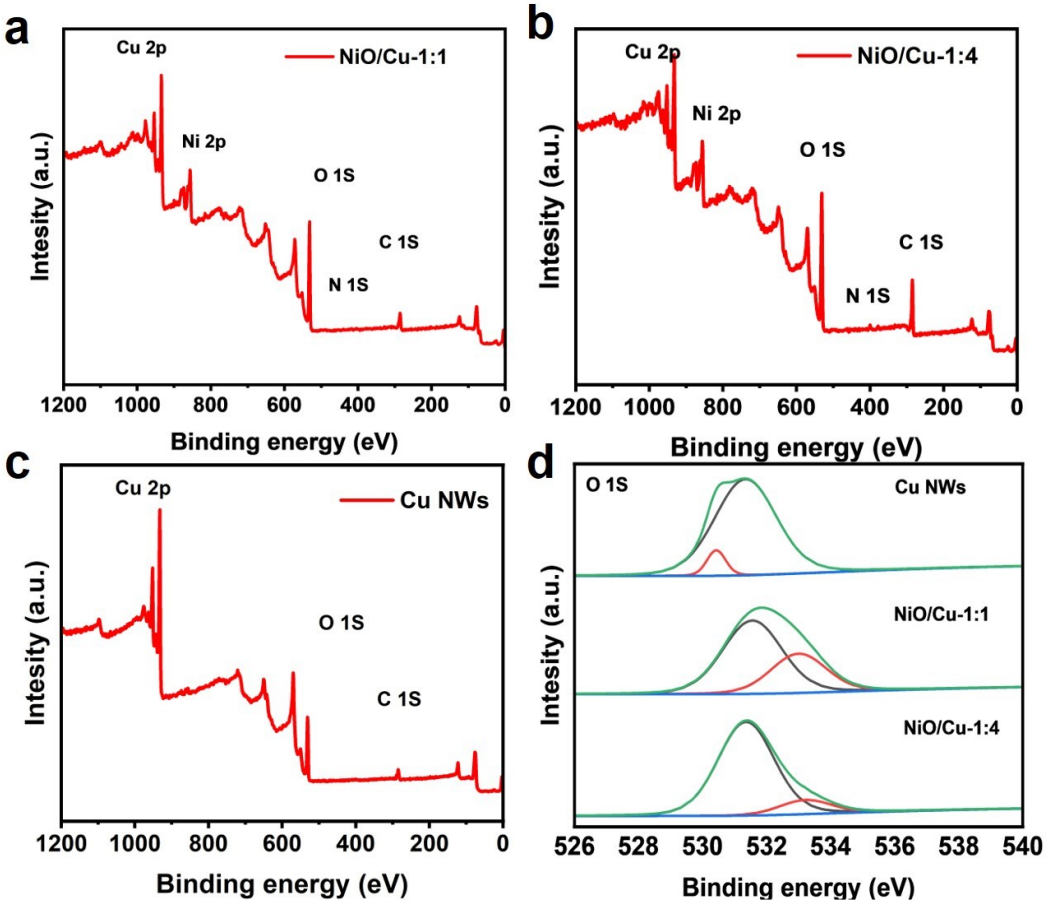

Figure S4. a-c) XPS spectra of NiO/Cu (1:1), NiO/Cu (1:1) and Cu NWs; d) O 1S XPS spectra of NiO/Cu (1:1), NiO/Cu (1:4) and Cu NWs.

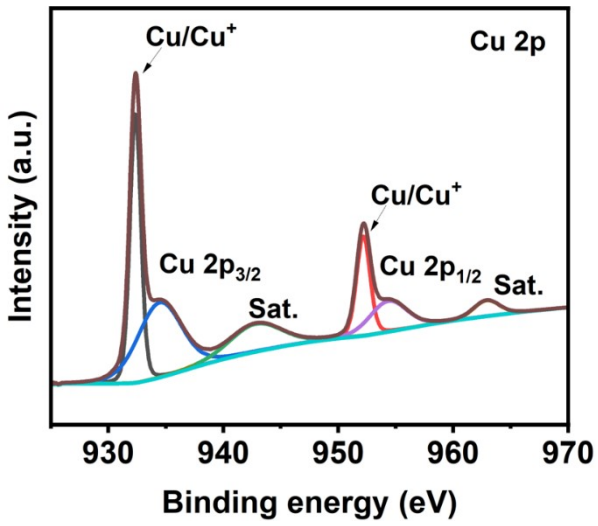

Figure S5. Cu 2*p* XPS spectrum of Cu NWs prepared by electro-reduction of CuO NWs.

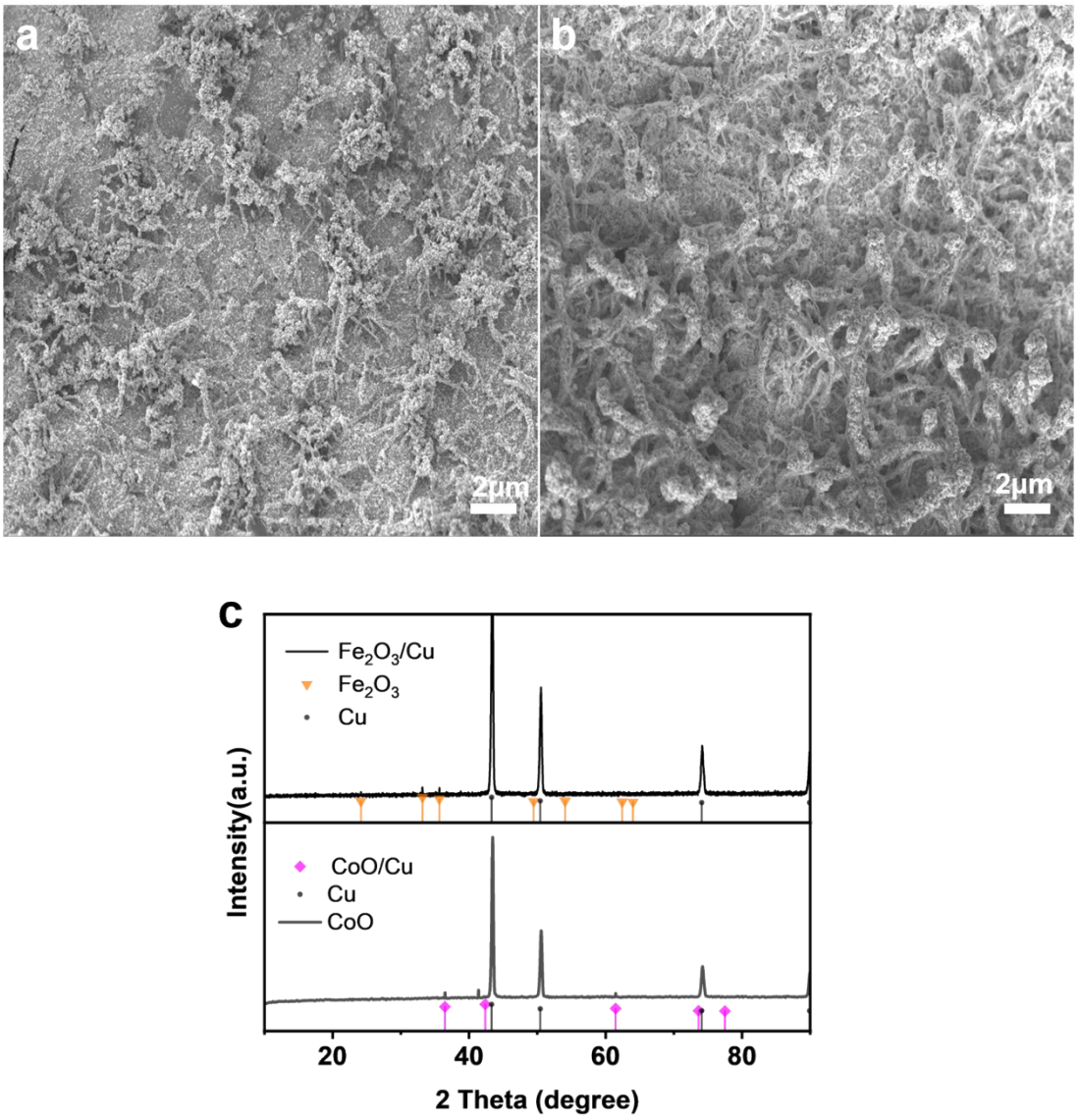

Figure S6. a) Fe_2O_3/Cu-1:1 composite catalyst obtained by electrodeposition and b) CoO/Cu-1:1 composite catalyst obtained by electrodeposition.c）XRD spectra corresponding to Fe_2O_3/Cu-1:1 and CoO/Cu-1:1.

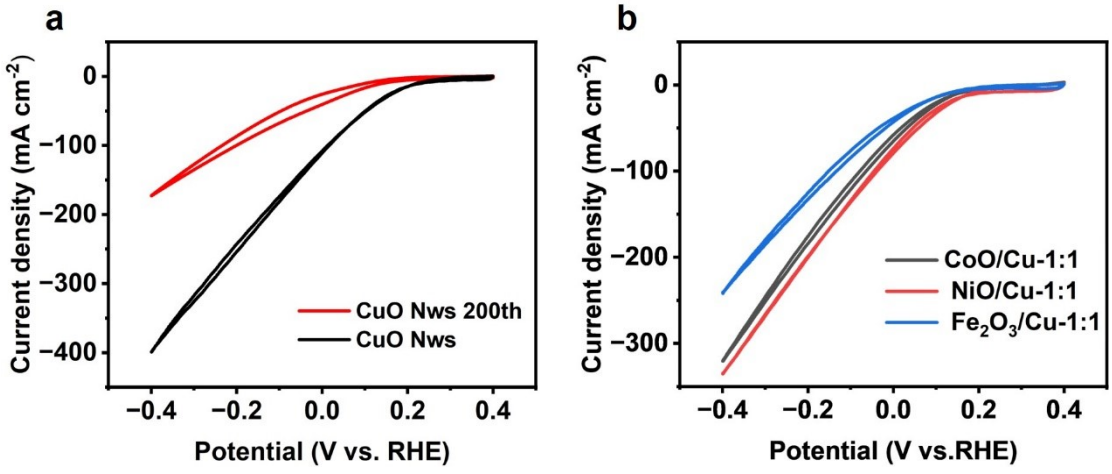

Figure S7. a) CV curves of CuO NWs in 1 M KOH electrolyte containing 0.1 M KNO_3 after 200 cycles. b) CV curves of different electrocatalysts in 1 M KOH electrolyte containing 0.1 M KNO_3 after 200 cycles (CoO/Cu-1:1, NiO/Cu-1:1 and Fe_2O_3/Cu-1:1).

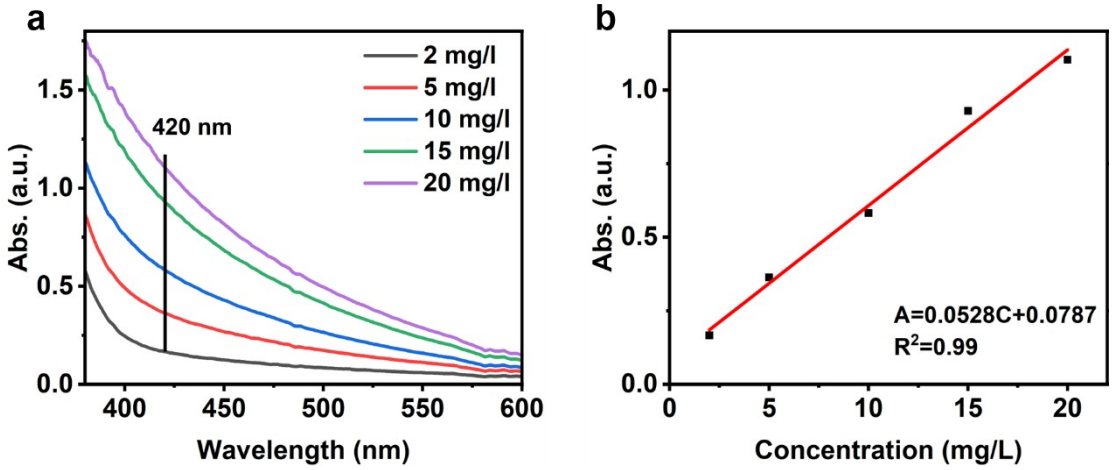

Figure S8. UV-Vis curves and calibration curves for determining NH_4^+. 1 mL NH_4Cl standard solution was diluted to 5 mL for test.

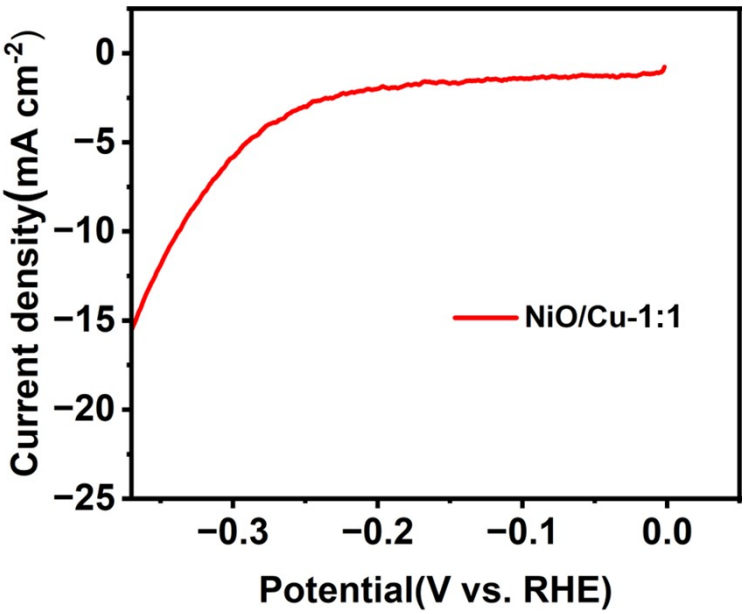

Figure S9. HER performance of NiO/Cu-1:1 catalyst.

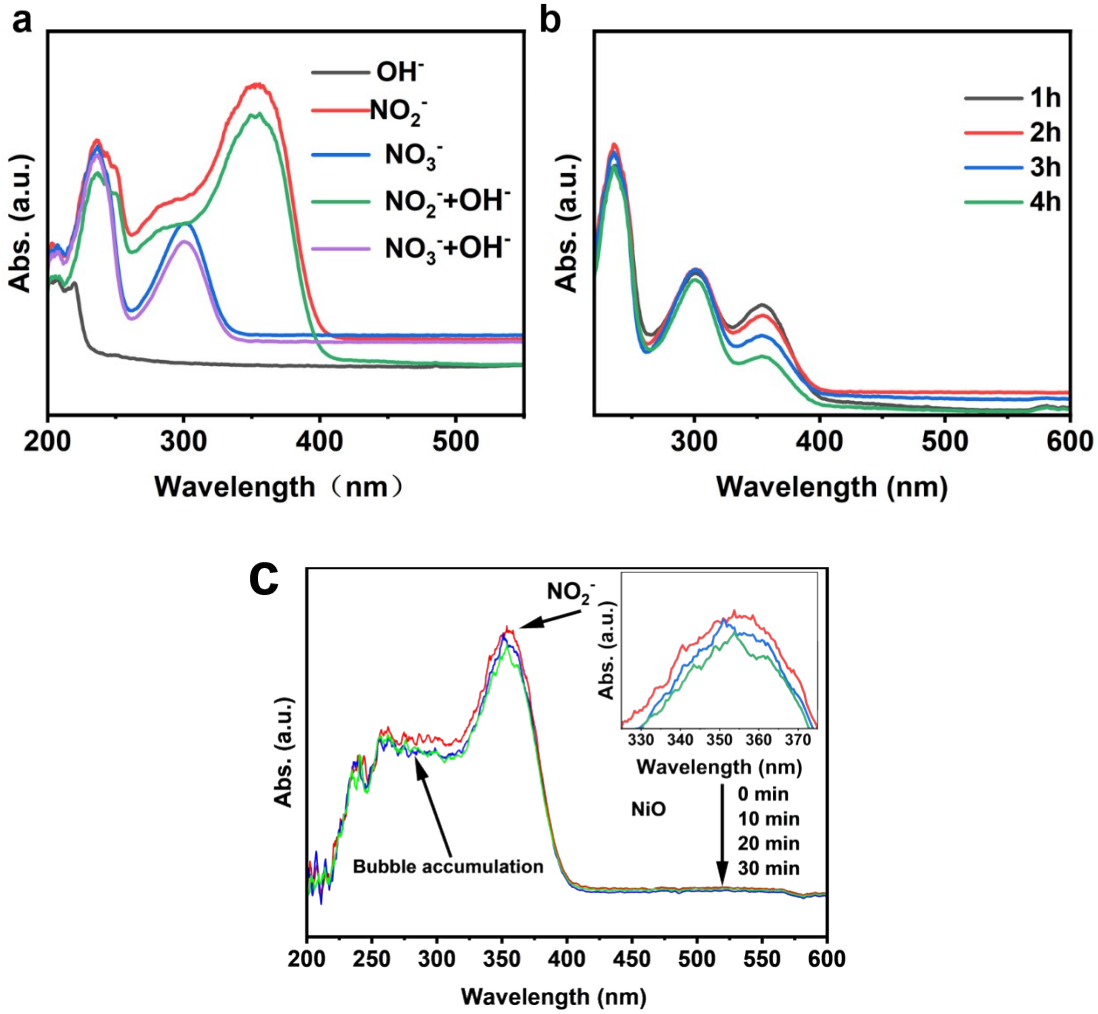

Figure S10. a) UV spectra for different kinds of anions. b) The four reaction cycles for the electrolytes detected by the UV spectrum. C) In situ ultraviolet–visible (UV–Vis) spectroscopy measurements of NO_2^- reduction on NiO NWs in 1 M KOH with 0.1 M KNO_2 electrolyte.

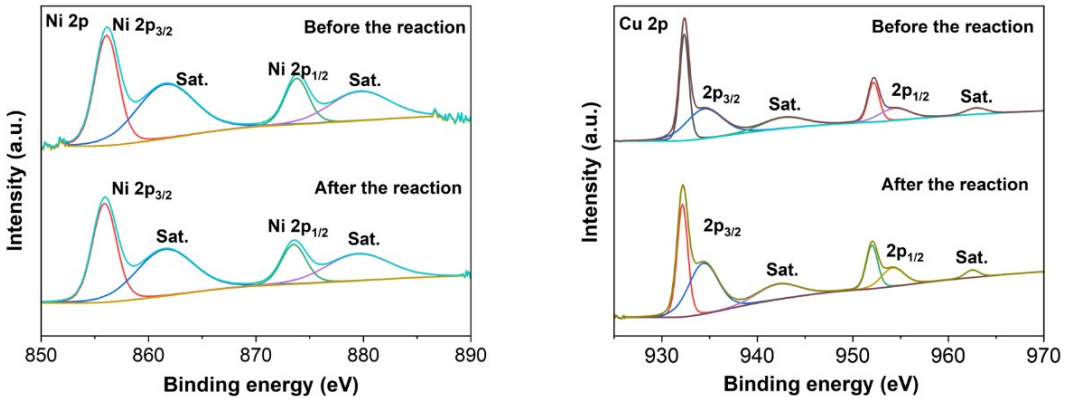

Figure S11. Ni and Cu 2*p* XPS spectra before and after the reaction.

Table S1 The standard reduction potentials of metals.

Reaction	Standard potential/V
Ni^{2+}/Ni	−0.257
Cu^{2+}/Cu	0.342

Table S2 Comparison of NO_3RR performance for some recently reported electrocatalysts in alkaline electrolytes.

Catalysts	Electrolytes	NH_3 yield rate	Faradaic Efficiency (%)	Reference
NiO/Cu/CF	1 M KOH + 0.1 M KNO_3	455 mg h^{-1} cm^{-2}@ −0.3 V vs. RHE	97	This work
CuCoSP	0.1M KOH +0.01M KNO_3	1.17mmol $cm^{-2}h^{-1}$ @ −0.175 V vs. RHE	92.8	Nat. Commun., 2022, 13, 1129.[1]
Cu/Cu_2O NWAs on Cu mesh	0.5 M Na_2SO_4 and 200 ppm NO_3^-	0.2449 mmol $cm^{-2}h^{-1}$@ -0.85 V vs. RHE	81	Angew. Chem. Int. Ed., 2020, 59, 5350-5354.[2]
Cu_2O Ar-40	0.5M Na_2SO_4 + 200 ppm NO_3^-	0.0699 mmol $cm^{-2}h^{-1}$@ − 1.2 V vs. Ag/AgCl	89.54	Applied Catalysis B: Environmental, 2022, 305, 121021.[3]
CuFe-450	1 M KOH + 100 mM HNO_3	30 mg $cm^{-2}h^{-1}$ @ −0.8 V vs. RHE	90.6	Chem Catalysis, 2022, [4]
Fe-cyano-RNSs	1 M KOH + 100 mM HNO_3	1.5mmol $cm^{-2}h^{-1}$ @ −0.6 V vs. RHE	90.2	ACS Nano, 2022, 2, 1072–1081.[5]
CoP NAs/CFC	1.0 M NaOH + 1.0 M $NaNO_3$	15.44 mol m^{-2} h^{-1}@ −0.6 V vs. RHE	~100	Energy Environ. Sci., 2022, 15, 760-770.[6]
CoO_x	0.1 M KOH +100 mM HNO_3	82.4 mg h^{-1} mg^{-1} cat @ -0.3 V vs. RHE	93.4	ACS Catal., 2021, 11, 15135-15140.[7]
Cu-NBs-100	1 M KOH + 0.1 M KNO_3	650 mmol g^{-1} $cath^{-1}$ @ -0.15 V vs. RHE	95	Energy Environ. Sci., 2021, 14, 4989-4997.[8]
R-NiCu-OH	1 M KOH + 0.1 M KNO_3	23 mg $cm^{-2}h^{-1}$ @ −0.1 V vs. RHE	72	Energy Environ. Sci., 2022, 15, 3004.[9]

TiO_{2-x}	50 ppm NO_3^- + 0.5 M Na_2SO_4	0.045 mmol h^{-1} cm^{-2} at −1.6 V vs. SCE	85	ACS Catal. 2020, 10, 3533-3540.[10]
Strained Ru nanoclusters	1 M KOH + 1 M KNO_3	1.17 mmol h^{-1} cm^{-2} at −0.8 V vs. RHE	100	J. Am. Chem. Soc. 2020, 142, 7036-7046.[11]
Ti foil	0.4M NO_3^- at pH~0.77		82	ACS Sustain. Chem. Eng. 2020, 8, 2672-2681.[12]
Copper-molecular solid catalyst	0.1 M PBS solution (pH7) contained 500 ppm NO_3^-	0.0514 mmol h^{-1} cm^{-2} at −0.6 V vs. RHE	85.9	Nat. Energy 2020, 5, 605-613.[13]
Copper-nickel alloys	1 M KOH containing 0.1 M KNO_3	170 mA cm^{-2} at −0.15 V vs. RHE using rotating disk electrodes at 100 rpm	99	J. Am. Chem. Soc. 2020, 142, 5702-5708.[14]
A single-site iron	0.1 M KOH containing 0.1 M KNO_3	0.161 mmol h^{-1} cm^{-2} at -0.7 V vs. RHE	nearly 100% after - 0.3 V vs. RHE	Energy Environ. Sci. 2021,14, 3522-3531.[15]
Fe single atom	0.50 M KNO_3/ 0.10 M K_2SO_4	0.46 mmol h^{-1} cm^{-2} at -0.85 V vs. RHE	~ 75	Nat. Commun. 2021, 12, 2870.[16]
Ru SA on N-doped carbon	0.05 M H_2SO_4 electrolyte	0.0018 mmol cm^{-2} h^{-1} at −0.2 V vs. RHE	29.6% at −0.2 V vs. RHE	Adv. Mater. 2018, 30, 1803498.[17]
Rh@Cu-0.6%	0.1 M Na_2SO_4 (pH 11.5) + 0.1 M KNO_3	1.27 mmol h^{-1} cm^{-2} at −0.4 V vs. RHE	93% at −0.2 V vs. RHE	Angew. Chem. Int. Ed. 2022, 61, e202202556.[18]

Table S3 Comparison of NO_3RR performance for Cu-based catalysts.

			Faradaic	

			Efficiency (%)	
CuCoSP	0.1M KOH +0.01M KNO_3	1.17mmol $cm^{-2}h^{-1}$ @ −0.175 V vs. RHE	92.8	Nat. Commun., 2022, 13, 1129.
Cu/Cu_2O NWAs on Cu mesh	0.5 M Na_2SO_4 and 200 ppm NO_3^-	0.2449 mmol $cm^{-2}h^{-1}$@ -0.85 V vs. RHE	81	Angew. Chem. Int. Ed., 2020, 59, 5350-5354.
Cu_2O Ar-40	0.5M Na_2SO_4 + 200 ppm NO_3^-	0.0699 mmol $cm^{-2}h^{-1}$@ − 1.2 V vs. Ag/AgCl	89.54	Applied Catalysis B: Environmental, 2022, 305, 121021.
CuFe-450	1 M KOH + 100 mM HNO_3	30 mg $cm^{-2}h^{-1}$ @ −0.8 V vs. RHE	90.6	Chem Catalysis, 2022,
Cu-NBs-100	1 M KOH + 0.1 M KNO_3	650 mmol g^{-1} $cath^{-1}$ @ -0.15 V vs. RHE	95	Energy Environ. Sci., 2021, 14, 4989-4997.
R-NiCu-OH	1 M KOH + 0.1 M KNO_3	23 mg $cm^{-2}h^{-1}$ @ −0.1 V vs. RHE	72	Energy Environ. Sci., 2022, 15, 3004.
Rh@Cu-0.6%	0.1 M Na_2SO_4 (pH 11.5) + 0.1 M KNO_3	1.27 mmol h^{-1} cm^{-2} at −0.4 V vs. RHE	93% at −0.2 V vs. RHE	Angew. Chem. Int. Ed. 2022, 61, e202202556.
NiO/Cu/CF	1 M KOH + 0.1 M KNO_3	455 mg h^{-1} cm^{-2}@ −0.3 V vs. RHE	97	This work

REFERENCES

1. W. He, J. Zhang, S. Dieckhofer, S. Varhade, A. C. Brix, A. Lielpetere, S. Seisel, J. R. C. Junqueira and W. Schuhmann, *Nat Commun*, 2022, **13**, 1129.
2. Y. Wang, W. Zhou, R. Jia, Y. Yu and B. Zhang, *Angew. Chem. Int. Ed. Engl.*, 2020, **59**, 5350-5354.
3. Z. Gong, W. Zhong, Z. He, Q. Liu, H. Chen, D. Zhou, N. Zhang, X. Kang and Y. Chen, *Appl. Catal., B*, 2022, **305**.
4. R. Hao, L. Tian, C. Wang, L. Wang, Y. Liu, G. Wang, W. Li and G. A. Ozin, *Chem Catalysis*, 2022, **2**, 622-638.
5. Z. Fang, Z. Jin, S. Tang, P. Li, P. Wu and G. Yu, *ACS Nano*, 2022, **16**, 1072-1081.
6. S. Ye, Z. Chen, G. Zhang, W. Chen, C. Peng, X. Yang, L. Zheng, Y. Li, X. Ren, H. Cao, D. Xue, J. Qiu, Q. Zhang and J. Liu, *Energy & Environ. Sci.*, 2022, **15**, 760-770.
7. J. Wang, C. Cai, Y. Wang, X. Yang, D. Wu, Y. Zhu, M. Li, M. Gu and M. Shao, *ACS Catalysis*, 2021, **11**, 15135-15140.
8. Q. Hu, Y. Qin, X. Wang, Z. Wang, X. Huang, H. Zheng, K. Gao, H. Yang, P. Zhang, M. Shao and C. He, *Energy & Environ. Sci.*, 2021, **14**, 4989-4997.
9. S. Li, P. Ma, C. Gao, L. Liu, X. Wang, M. Shakouri, R. Chernikov, K. Wang, D. Liu, R. Ma and J. Wang, *Energy & Environ. Sci.*, 2022, **15**, 3004-3014.
10. R. Jia, Y. Wang, C. Wang, Y. Ling, Y. Yu and B. Zhang, *ACS Catalysis*, 2020, **10**, 3533-3540.
11. J. Li, G. Zhan, J. Yang, F. Quan, C. Mao, Y. Liu, B. Wang, F. Lei, L. Li, A. W. M. Chan, L. Xu, Y. Shi, Y. Du, W. Hao, P. K. Wong, J. Wang, S. X. Dou, L. Zhang and J. C. Yu, *J Am Chem Soc*, 2020, **142**, 7036-7046.
12. I. Katsounaros, *Curr Opin Electrochem*, 2021, **28**.
13. G.-F. Chen, Y. Yuan, H. Jiang, S.-Y. Ren, L.-X. Ding, L. Ma, T. Wu, J. Lu and H. Wang, *Nature Energy*, 2020, **5**, 605-613.
14. Y. Wang, A. Xu, Z. Wang, L. Huang, J. Li, F. Li, J. Wicks, M. Luo, D. H. Nam, C. S. Tan, Y. Ding, J. Wu, Y. Lum, C. T. Dinh, D. Sinton, G. Zheng and E. H. Sargent, *J Am Chem Soc*, 2020, **142**, 5702-5708.
15. P. Li, Z. Jin, Z. Fang and G. Yu, *Energy & Environ. Sci.*, 2021, **14**, 3522-3531.
16. Z. Y. Wu, M. Karamad, X. Yong, Q. Huang, D. A. Cullen, P. Zhu, C. Xia, Q. Xiao, M. Shakouri, F. Y. Chen, J. Y. T. Kim, Y. Xia, K. Heck, Y. Hu, M. S. Wong, Q. Li, I. Gates, S. Siahrostami and H. Wang, *Nat Commun*, 2021, **12**, 2870.
17. Z. Geng, Y. Liu, X. Kong, P. Li, K. Li, Z. Liu, J. Du, M. Shu, R. Si and J. Zeng, *Adv Mater*, 2018, e1803498.
18. H. Liu, X. Lang, C. Zhu, J. Timoshenko, M. Ruscher, L. Bai, N. Guijarro, H. Yin, Y. Peng, J. Li, Z. Liu, W. Wang, B. R. Cuenya and J. Luo, *Angew. Chem. Int. Ed. Engl.,* 2022, **61**, e202202556.